

Express Mail No.: EL622259195US

Date of Deposit: January 3, 2002

APPLICATION FOR UNITED STATES LETTERS PATENT
FOR
POTENTIOMETRIC NO_x SENSORS BASED ON YTTRIA-STABILIZED
ZIRCONIA WITH ZEOLITE MODIFIED ELECTRODE

Inventors: Prabir K. Dutta
Nicholas F. Szabo
Hongbin Du
Sheikh A. Akbar

Assignee: The Ohio State University

Attorney: Roger A. Gilcrest
Standley & Gilcrest, LLP
495 Metro Place South, Suite 210
Dublin, Ohio 43017-5315
Telephone: (614) 792-5555
Facsimile: (614) 792-5536

Potentiometric NO_x Sensors Based on Yttria-Stabilized Zirconia with Zeolite Modified Electrode

Inventors: Prabir K. Dutta
Nicholas F. Szabo
Hongbin Du
Sheikh A. Akbar

[0001] The present invention was made with Government support under Grant No. EEC-9523358 awarded by the National Science Foundation. The United States Government may have certain rights to this invention under 35 U.S.C. §200 et seq.

TECHNICAL FIELD OF INVENTION

[0002] The present invention relates to nitrogen oxide (NO_x) measurement systems for use in harsh environments. The present invention provides sensors based on the solid electrolyte yttria stabilized zirconia (YSZ) with platinum (Pt) electrodes where one electrode is modified by a zeolite NaY coating.

BACKGROUND OF THE INVENTION

[0003] Due to a continuing need for the development of rugged and reliable sensors capable of taking measurements in harsh industrial environments, there has been extensive research in this area as evidenced by the technical literature.

[0004] For example, Yamazoe *et al.* has reported a series of sensors based on stabilized zirconia with mixed metal oxide electrode systems. A CdCr₂O₄ attached device was reported as a good potentiometric sensor for NO_x gases in the temperature range of 500 to 600 °C. In several other papers, they have studied different metal oxide systems and found CdMn₂O₄ as a good candidate for sensing applications. They have also proposed a NO_x sensing mechanism involving mixed potential based on the measurements of polarization curves.

[0005] Lu *et al.* has recently reported the study of YSZ (yttria stabilized zirconia) based sensors using a tungsten tri-oxide (WO_3) electrode for the detection of NO and NO_2 . The EMF response of the WO_3 -attached device is nearly linear to the logarithm of NO or NO_2 concentrations. Kurosawa *et al.* has fabricated a NO_x sensor based on MgO stabilized zirconia with an auxiliary phase of $\text{Ba}(\text{NO}_3)_2$. E.L. Brosha *et al.* has reported mixed potential sensors based on dense, thin films of lanthanum cobaltate pervoskites for carbon monoxide (CO) and hydrocarbon gases. R. Mukundan *et al.* has studied mixed potential YSZ and CeGdO_x based sensors with platinum (Pt) and gold (Au) electrodes for hydrocarbon and CO sensing measurements. According to them, a CeGdO_x based sensor gave a more stable and reproducible response than a YSZ electrolyte due to the better oxygen reduction kinetics of metal electrodes on ceria-based electrolytes. The same group has reported that the reproducibility of the response behavior was dependent of Au morphology. T. Hibino *et al.* has reported non-Nernstian behavior at tantalum oxide modified Au electrodes for hydrocarbon sensing.

[0006] Zeolites have recently become the subject of considerable research in sensor applications. In the past 15 years there has been considerable research done on zeolite modified electrodes (ZMEs), the study of putting a layer containing zeolite particles onto an electrode surface. Walcarius classifies five main applications of ZMEs, which include electrocatalysis, electroanalysis, charge storage devices, molecular recognition, and mass transport characterization. For utilization in sensor materials, electroanalysis is of particular importance. Walcarius subdivides this application into the five categories of direct detection, indirect detection, amperometric biosensors, potentiometric analysis, and voltametry after preconcentration. Various methods have been used to cover the electrode such as

zeolite dispersion in a binder, pressing zeolite powder onto the electrode, applying a coating of the zeolite in a polymer matrix, and covalently linking zeolite to the surface of the electrode. The majority of electroanalysis applications using ZMEs have been for determination of species, usually metal cations, in the liquid phase.

[0007] There have been few accounts of using zeolite materials for gas phase sensing at various temperatures and conditions. One design studied is a sensor operating at 300 °C for the detection of CO using SnO₂ coated onto a platinum wire. The SnO₂ is impregnated with Au-La₂O₃ and this layer is subsequently covered with a layer of the zeolite ferrierite. The addition of the zeolite serves as a catalyst filter to allow selectivity for CO in the presence of H₂, CH₄, C₂H₄, i-C₄H₁₀ and C₂H₅OH.

[0008] Au-NaY zeolite electrodes are used to monitor ethanol and ammonia vapors using cyclic voltametry. High current densities are obtained in the presence of ethanol and ammonia vapors at 25 °C.

[0009] Zeolites deposited on a quartz crystal microbalance (QCM) are used as sensors for gaseous molecules. Cu-ZSM-5 zeolite is deposited onto a quartz substrate with a gold (Au) electrode and used to detect NO in helium (He) at 384K. The shift of the fundamental resonance frequency of the QCM was found to be proportional to the amount of NO present. A similar study done at 423K involving a thin layer of the zeolite faujasite on a QCM with Au electrodes detected SO₂ in the presence of O₂. Other studies involving sensor based systems include: the use of zeolites in amperometric biosensors for H₂O₂ and glucose oxidase, NH₃ detection by monitoring the change of conductivity of zeolite Na⁺ beta and H⁺ beta measured by impedance spectroscopy, use of the zeolite NaY-(Ru²⁺(bpy)₃) as a fluorescence O₂ sensor, and for gas detection by micromechanical cantilevers attached with zeolite crystals at the apex.

[0010] There is a continuing need for the development of rugged and reliable sensors capable of making measurements in the harsh industrial environments found in the steel, heat treating, metal casting, glass, ceramic, pulp and paper, automotive, aerospace, and utility and power industries. The 1990 Clean Air Act amendments (CAAA) will require many power and utility industries to monitor emissions. Emission monitoring sensors for these applications include those for CO, NO_x, O₂ and hydrocarbons. Combustion engines are a major contributor of NO_x emissions. The major species of NO_x in automotive exhaust gases are NO, NO₂ and N₂O of which 90% of the total amount is NO. Nitrogen oxides can be toxic to humans, with possible lung impairment due to exposure of less than 15 ppm NO₂. It is therefore imperative to develop a sensor for NO_x that will provide real time analysis for engine control and onboard diagnostics to monitor and control these emissions.

SUMMARY OF THE INVENTION

[0011] The present invention presents a novel potentiometric sensor.

[0012] A potentiometric sensor of the present invention comprises an alumina tube having an interior and an exterior. A cap member closes one end of the tube. The cap member has an interior surface exposed to the interior of the alumina tube and an exterior surface. The cap member comprises yttria-stabilized zirconia. A first electrode is disposed on the interior surface of the cap member. The first electrode is covered by zeolite. The zeolite is in the interior of the alumina tube. A second electrode is disposed on the exterior surface of the cap member.

[0013] It is preferred that a potentiometric sensor of the present invention additionally comprise a measurement apparatus (potentiometer) that measures the

electrical potential between the first and second electrodes disposed on the sensor. Further, it is preferred that the first electrode, second electrode or both electrodes comprise a material selected from the group consisting of platinum, gold and Cr_2O_3 . Additionally, it is preferred that the zeolite is Zeolite Y.

[0014] A second embodiment of a sensor of the present invention is a potentiometric sensor comprising a tube having an exterior and an interior. The tube comprises yttria-stabilized zirconia. A first electrode is disposed of the exterior of the tube and a second electrode is disposed on the interior of the tube. A zeolite material covers one of the electrodes.

[0015] It is preferred that a potentiometric sensor of the present invention additionally comprise a measurement apparatus (potentiometer) that measures the electrical potential between the first and second electrodes disposed on the tube. Further, it is preferred that the first electrode, second electrode or both electrodes comprise a material selected from the group consisting of platinum, gold and Cr_2O_3 . Additionally, it is preferred that the zeolite is Zeolite Y.

[0016] A third embodiment of a sensor of the present invention is a potentiometric sensor comprising a substrate. The substrate comprises yttria-stabilized zirconia. A first electrode is disposed on the substrate. A second electrode is disposed on the substrate and covered with a layer of zeolite. The electrodes may be disposed on the same side of the substrate or may be placed on opposite surfaces of the substrate.

[0017] It is preferred that a potentiometric sensor of the present invention additionally comprise a source of an electrical potential supplied to the electrodes and a potentiometer in electrical contact with the source of electrical potential. Further, it is preferred that the first electrode, the second electrode or both

electrodes comprise a material selected from the group consisting of platinum, gold and Cr_2O_3 . Additionally, it is preferred that the zeolite is Zeolite Y.

[0018] In a most preferred Type 3 sensor embodiment of the present invention, a porous member may shield the substrate and the first and second electrodes from the harsh exhaust gas environment. The porous member prevents the exhaust gas from directly contacting the substrate and the first and second electrodes. The exhaust gas can come in contact with these elements only after traveling through the porous member. In this way, the porous member prevents degradation of the sensitive underlying elements such as the substrate, first electrode and second electrode.

BRIEF DESCRIPTION OF THE DRAWINGS

[0019] Novel features and advantages of the present invention, in addition to those mentioned above, will become apparent to those skilled in the art from a reading of the following detailed description in conjunction with the accompanying drawings wherein similar reference characters refer to similar parts and in which:

[0020] Figure 1 shows a sensor (Type 1) of the present invention.

[0021] Figure 2 shows a sensor (Type 2) of the present invention.

[0022] Figure 3 shows a sensor (Type 3) of the present invention.

[0023] Figure 4 shows a schematic of an exhaust sensor (Type 3) assembly of the present invention.

[0024] Figure 5 is a picture of an exhaust sensor assembly of the present invention.

[0025] Figure 6 is a diagram of an experimental testing apparatus.

- [0026] Figure 7 compares the response of an uncoated Type 3 sensor with a NaY coated Type 3 sensor for 0 – 800 ppm NO in 3% O₂.
- [0027] Figure 8 illustrates a typical Type I sensor output to NO concentration.
- [0028] Figure 9 is a graph showing sensitivity plots for the three types of sensors of the present invention.
- [0029] Figure 10 shows the reproducibility of Type III sensor performance.
- [0030] Figure 11 depicts a YSZ closed-end tube type sensor with an air reference.
- [0031] Figure 12 is a graph of the NO calibration curves for the sensor shown in Figure 11.
- [0032] Figure 13 illustrates the NO calibration curve for a zeolite-based Type 2 sensor.
- [0033] Figure 14 shows the calibration curves obtained with CO using a Type 2 sensor when exposed to different O₂ concentrations.
- [0034] Figure 15 illustrates the sensor response to both CO and NO in 21% O₂.
- [0035] Figure 16 compares the potentiometric response of a Type 3 sensor to 400 ppm NO and 400 ppm NO + 100 ppm NO₂ in 3% O₂ at 500 °C.
- [0036] Figure 17 shows the experimental apparatus used to test the automotive sensor probe shown in Figures 4 and 5.
- [0037] Figure 18 shows a typical NO emission profile as measured by IR.
- [0038] Figure 19 shows the output of the NO sensor.

DETAILED DESCRIPTION OF THE PREFERRED EMBODIMENT(S)

[0039] Three sensor designs based upon the same principle are disclosed.


The first sensor **10** (Type 1), shown in Figure 1, is comprised of a YSZ pressed pellet **12** with a first platinum (Pt) electrode **14** and a second platinum electrode **16** mounted onto an alumina tube **18** packed with zeolite NaY (LZY-52 from Union Carbide) **19**. The YSZ pellet was constructed from commercially available YSZ powder (HSY-8, Zirconia Sales Inc., 8 mol% YSZ). The pellet was formed in a stainless steel die (Carver Inc.) under 10,000 psi on a Carver pellet press. The green pellet was put onto an alumina plate and sintered in a Lindberg Blue high temperature box furnace at 1450 °C for 6 hours with 6 °C/min heating and cooling rates. The final pellet dimensions were approximately 9 mm in diameter and 2 mm thick. The pellet was white in color. Pt ink (Englehard Corporation, lot #A47331) was painted on both sides of the pellet and Pt lead wires (Englehard Corporation, 31 AWG) were set into the wet Pt ink. The ink was then cured in a Lindberg Blue box furnace at 1250 °C for 2 hours with a heating and cooling rate of 6 °C/min. The resulting electrodes had a metallic grey color. The pellet was then mounted onto an alumina tube (Coors Ceramic), approximately 1 inch in length, with a high temperature inorganic adhesive, Ceramabond 569 (Aremco). Thus, one lead wire was on the outside of the tube and the other wire on the inside. The Ceramabond was then left to dry for 1 – 2 hours at room temperature. The purpose of the tube is to hold zeolite powder, which was then packed on the inside as to cover the electrode. After final assembly, the sensor was put into a tube furnace at 500 °C for a few hours to thermally stabilize it before testing.

[0040] The second sensor **20** (Type 2), shown in Figure 2, comprises a cylindrical piece of 8 mol% YSZ **22** (Vesuvius McDanel), approximately 20 mm length, 6 mm outside diameter, 4.5 mm inside diameter, cut with a diamond saw

(Leco). Pt electrodes **24** and **26** were prepared in a similar manner as the type 1 design. After the sensor body was prepared, zeolite NaY powder **29** was packed into the inside as to cover the inside electrode **26**. The final sensor was then heated at 500 °C in a tube furnace to achieve thermal equilibrium before testing.

[0041] The third sensor **30** (Type 3), shown in Figure 3, comprises a YSZ pellet **32** with two Pt electrodes **34** and **36** on the same side (planar structure) with one of the Pt electrodes coated by a layer of zeolite **39**. The YSZ pellet and electrodes were prepared using the same materials and methods as the Type 1 design. A viscous zeolite paste was prepared by mixing zeolite NaY powder with terpeneol solvent. The paste was applied with a paint brush over one of the Pt electrodes. After the paste application, the sensor was heated in a tube furnace at 500 °C for 2 hours to evaporate the terpeneol solvent and stabilize the coating.

[0042] The interest in NO sensors arises because of their possible utility in sensing gases in high temperature combustion processes. Of particular interest to the community is sensing NO emissions from automotive engines. Because of the high temperatures and the presence of high flow rates and particulates in the exhaust, the sensor needs appropriate packaging. The planar sensor (Type 3) lends itself to a possible packaging design that can survive harsh environments. Figure 4 shows a schematic of how the planar sensor (Type 3) has been incorporated into a spark plug tube. The assembly **40** is subjected to an exhaust gas stream **41**. The exhaust gas stream **41** flows over the exposed porous cap **43**. The porous cap **43** protects the electrodes **44**, **49** from the harsh environment of the exhaust gas stream **41** while permitting the exhaust gas to contact the electrodes. Any suitable material may be used for the porous cap **43** provided that it allows the exhaust gas to contact the electrodes and also protects the electrodes from degradation caused by the



harsh exhaust gas environment. The electrodes are each disposed on a YSZ substrate **42**. Lead wires **45** connect the electrodes to a potentiometer. Figure **5** shows an actual picture of the sensor assembly. To improve the mechanical stability of the zeolite layer in a high flow environment a zeolite pellet was placed on top of the zeolite powder and bonded to the YSZ pellet around the edges with Ceramabond.

[0043] Gas sensing experiments were performed within a quartz tube located inside a high temperature tube furnace (Lindberg Blue model) shown in Figure **6**. The sensor rested in a quartz tube while the two sensor wires were connected to two Pt wires threaded into the quartz tube, which led outside the furnace. The tube furnace **64** was used to heat and cool the sensor **65** at a programmed rate as well as maintaining it at a temperature between 500 – 700 °C, depending upon the experiment. Air **68**, N₂ **67** and combustion gases **69** such as NO (2000 ppm source tank), NO₂ (1000 ppm source tank) and CO (2000 ppm source tank) were metered through Sierra brand mass flowmeters **66** to form gas mixtures of various compositions, with a volumetric flow rate of 100 cc/min. The voltage output of the sensor response to changes in the gas concentrations were monitored by a Hewlett Packard multimeter **62** (34401A) and recorded by Hewlett Packard Benchlink software on a Windows 95 Pentium based PC **61**.

[0044] The three sensor types and the automotive exhaust probe were tested and the results are outlined below.

[0045] Figures **1**, **2** and **3** show the sensor designs that were investigated. In developing these designs, the strategy is to build asymmetry between the two Pt electrodes by covering one of the electrodes with zeolite NaY. Figure **7** compares the response of an uncoated (no NaY coating) Type 3 sensor and a NaY coated

Type 3 sensor for 0 – 800 ppm NO in 3% O₂. It is evident that the presence of NaY causes an enhanced signal toward NO. All three types of sensors showed similar behavior towards NO, as demonstrated in Figure 8 for a tubular (Type 1) design. Because of the asymmetry provided by the zeolite layer, it becomes possible to expose the complete sensor to the sensing gases without the need for an air reference. Figure 9 compares the sensitivity plots for the three designs. The voltage follows a linear dependence with the logarithm of the NO concentration. The reproducibility of sensor performance is for data obtained from three planar sensors where the signal variation for one standard deviation is shown in Figure 10. The variations are likely due to factors in the fabrication process, including the size and thickness of the Pt electrodes, and the zeolite film thickness and packing.

[0046] Next, interference effects will be explored.

[0047] Since YSZ is an oxygen ion conductor, any imbalance of O₂ on two Pt electrodes will alter the baseline. This is demonstrated by using a YSZ closed-end tube type sensor 110 (see Figure 11) having two Pt electrodes 116 with an air reference 112 where the oxygen inside the YSZ tube 114 is at 21%, whereas the outside of the sensor is exposed to NO 118 (100 – 1000 ppm) at varying oxygen levels similar to a combustion environment. Figure 12 shows the NO calibration curves for this sensor. If a similar experiment is done with a zeolite-based sensor (e.g., a Type 2 as shown in Figure 2), the calibration curve collapse to approximately the same line (Figure 13), demonstrating that the level of O₂ at both Pt electrodes is similar, primarily because the microporosity of the zeolite allows for O₂ transport to the underlying Pt electrode. Another manifestation of the same effect can be seen in Figure 7 with the planar sensor (Type 3) where changing O₂ levels does not alter the background signal.

[0048] Figure 14 shows the calibration curves obtained with CO using sensor type 2 and its dependence on the O₂ concentration of the background gas. There is a strong signal from CO due to the electrochemical reaction $\text{CO} + \text{O}^{2-} \rightarrow \text{CO}_2 + 2\text{e}^-$. However, the slope of the calibration curve, which is a measure of sensitivity, decreases with increasing O₂ concentration. Figure 15 shows the sensor trace to both CO and NO in 21 % O₂, where the sensor appears to be almost insensitive to CO. The gradual decrease in CO signal with O₂ is because the CO gets oxidized on the Pt surface at the higher background O₂ levels, before it can reach the Pt-YSZ interface for the electrochemical reaction and the oxidation product CO₂ is electrochemically inactive.

[0049] Figure 16 compares the potentiometric response of a planar sensor (Type 3) to 400 ppm NO and 400 ppm NO + 100 ppm NO₂ in 3% O₂ at 500 °C. It is clear that in the presence of NO₂, the signal for NO is considerably diminished, indicating significant interference.

[0050] Using a Type 1 sensor, as shown in Figure 1, we measured the NO response in a fixed O₂ concentration (5%) at temperatures varying from 500 – 700 °C. This temperature range was chosen because YSZ begins to show significant ionic conduction only above 450 °C and zeolite Y retains a crystalline structure up to 750 °C. It was observed that the sensitivity of the sensor decreased with increasing temperature with virtually no sensor response at 700 °C. Two possible reasons for the diminished sensor sensitivity are preferential oxidation of NO at the Pt surface rather than at the Pt-YSZ boundary at higher temperatures, and also diminished adsorption of NO at the triple points on the Pt-YSZ at higher temperatures. This temperature dependence is consistent with previous measurements, e.g. on CdCr₂O₄ electrodes on YSZ, significant loss of sensitivity at 600 °C was reported.

[0051] The automotive sensor probe shown in Figures 4 and 5 was tested in an automotive engine set up 170 as shown in Figure 17. The automotive engine set up 170 comprises a dyno 171 connected to an engine 174. A sensor 173 is disposed in the exhaust stream of the engine. The gas flow direction is indicated by 177. An online IR analyzer 175 was used to verify the sensor response. The level of NO in the emission was altered by adjusting the engine speed and a typical NO emission profile as measured by the IR is shown in Figure 18. The output of the NO sensor is plotted in Figure 19 and the peaks follow a similar time profile as the IR output (see Figure 18, event 2, where no response of the NO sensor is observed). These preliminary data are encouraging, in that the sensor packaging survived repeated tests. The response time of the sensor is comparable to that of the IR detector. There is a delay in the response of the IR due to the length of the gas transfer line, which accounts for the small absolute time difference in the sensor and IR signals. The temperature of the exhaust stream fluctuated as the engine speed was altered and could be responsible for the changing backgrounds. Heating of the YSZ to minimize the effect of the temperature fluctuations is currently being investigated.

[0052] While the invention has been described in connection with what is presently considered to be the most practical and preferred embodiment, it is to be understood that the invention is not to be limited to the disclosed embodiment, but on the contrary, is intended to cover various modifications and equivalent arrangements included within the spirit and scope of the appended claims, which are incorporated herein by reference.

REFERENCES

1. N. Miura, G. Lu and N. Yamazoe, *Sensors and Actuators B*, 52 (1998) 169- 178.
2. N. Miura, H. Kurosawa, M. Hasei, G. Lu and N. Yamazoe, *Solid State Ionics*, 86-88 (1996) 1069-1073.
3. N. Miura, G. Lu, N. Yamazoe, H. Kurosawa and M. Hasei, *J. Electrochem. Soc.* 143 (2) (1996) L33 – L35.
4. G. Lu, N. Miura and N. Yamazoe, *Sensors and Actuators B*, 65 (2000) 125 – 127.
5. H. Kurosawa, Y. Yan, N. Miura and N. Yamazoe, *Solid State Ionics*, 79 (1995) 338-343.
6. E.L. Brosha, R. Mukundan, D.R. Brown, F.H. Garzon, J.H. Visser, M.Zanini, Z. Zhou and E.M. Logothetis, *Sensors and Actuators B*, 69 (2000) 171-182.
7. R. Mukundan, E.L. Brosha, D.R. Brown and F.H. Garzon, *Electrochemical and Solid State Letters*, 2(8) (1999) 412-414.
8. R. Mukundan, E.L. Brosha, D.R. Brown and F.H. Garzon, *J. Electrochem. Soc.* 147 (4) (2000) 1583-1588.
9. T. Hibino, S. Kakimoto and M. Sano, *J. Electrochem. Soc.* 146 (9) (1999) 3361-3366.
10. A. Walcarius, "Zeolite-Modified Electrodes in Electroanalytical Chemistry", *Analytical Chimica Acta*, 384, pp. 1 – 16 (1999).
11. A. Walcarius, "Factors Affecting the Analytical Applications of Zeolite Modified Electrodes: Indirect Detection of Nonelectroactive Cations", *Analytical Chimica Acta*, 388, pp. 79-91 (1999).
12. K. Fukui, S. Nishida, "CO Gas Sensor Based on Au-La₂O₃ Added SnO₂ Ceramics with Siliceous Zeolite Coat", *Sensors and Actuators B*, 45, pp. 101 – 106 (1997).
13. H. Tsuchiya, I. Sasaki, A. Harano, T. Okubo and M. Sadakata, "Zeolite Sensor for Nitrogen Monoxide Detection at High Temperature", *Mat. Res. Soc. Symp. Proc.*, 454, pp. 297-302 (1997).
14. O. Enea, "Morphological and Electrocatalytic Properties of Gold Deposits on NaY Zeolite", *Electrochim. Acta.*, pp. 1647-1654 (1989).
15. M. Osada, I. Sasaki, M. Nishioka, M. Sadakata, T. Okubo, "Synthesis of a Faujasite Thin Layer and its Application for SO₂ Sensing at Elevated Temperatures", *Microporous and Mesoporous Materials*, 23, pp. 287 – 294 (1998).
16. B. Liu, F. Yang, J. Kong, J. Deng, "A Reagentless Amperometric Biosensor Based on the Coimmobilization of Horseradish Peroxidase and Methylene Green in a Modified Zeolite Matrix", *Analytica Chimica Acta*, 386, pp. 31- 39 (1999).

17. U. Kunzellman, H. Bottche, "Biosensor Properties of Glucose Oxidase Immobilized Within SiO₂ Gels", *Sensors and Actuators B*, 39, pp. 222 – 228 (1997).
18. U. Simon, U. Flesch, W. Maunz, R. Muller, C. Plog, "The effect of NH₃ on the Ionic Conductivity of Dehydrated Zeolites Nabeta and Hbeta", *Microporous and Mesoporous Materials*, 21, pp. 111-116 (1998).
19. O.S. Wolfbeis, "Novel Oxygen Sensor Material Based on a Ruthenium Bipyridyl Complex Encapsulated in ZeoliteY: Dramatic Differences in the Efficiency of Luminescence Quenching by Oxygen on Going From Surface-Absorbed to Zeolite-Encapsulated Fluorophores", *Sensors and Actuators B*, 29, pp. 240 – 245 (1995).
20. R. Berger, Ch. Gerber, H.P. Lang, J.K. Gimzewski, "Micromechanics: A Toolbox for Femtoscale Science: Towards a Laboratory on a Tip", *Microelectronic Engineering*, 35, pp. 373-379 (1997).
21. L. Scandella, G. Binder, T. Mezzacasa, J. Gobrecht, R. Berger, H.P. Lang, Ch. Gerber, J.K. Gimzewski, J.H. Koepler, J.C. Jansen, "Combination of Single Crystal Zeolites and Microfabrication: Two Applications Toward Zeolite Nanodevices", *Microporous and Mesoporous Materials*, 21, pp. 403 – 409 (1998).

The aforementioned references are hereby incorporated herein by reference.